



4<sup>th</sup> IASPEI / IAEE International Symposium:

## Effects of Surface Geology on Seismic Motion

August 23–26, 2011 • University of California Santa Barbara

# A PREDICTIVE EQUATION FOR THE VERTICAL-TO-HORIZONTAL RATIO OF GROUND-MOTION AT ROCK SITES BASED ON SHEAR WAVE VELOCITY PROFILES

### Benjamin Edwards

Swiss Seismological Service, ETH  
8092 Zürich  
Switzerland

### Valerio Poggi

Swiss Seismological Service, ETH  
8092 Zürich  
Switzerland

### Donat Fäh

Swiss Seismological Service, ETH  
8092 Zürich  
Switzerland

### ABSTRACT

Ratios of vertical-to-horizontal (V/H) ground-motion are important for the computation of scenario compatible vertical design spectra. They are therefore a crucial aspect of seismic hazard analysis. We characterize the V/H ratio at rock sites in terms of the recording site's average quarter-wavelength velocity. A predictive equation is presented, which can be used for reconstructing the expected V/H ratio of the 5% damped response spectra for rock sites, given a known shear-wave velocity profile. We analyze well characterized hard rock sites in Switzerland using small earthquakes ( $M_w > 2$ ), whilst the magnitude range is increased up to events of  $M_w = 7.3$  using strong-motion recordings from Japan's KiK-Net seismic network. It is shown that a correlation between quarter-wavelength velocity at a given frequency and the V/H ground-motion ratio exists. Small differences, possibly due to velocity measurement bias or topographical and basin effects existed when analyzing the individual regional datasets. Apart from near-source distances ( $R < 30$  km), no clear magnitude- or distance-dependence of the V/H ratios is present. Keywords: V/H Ratio; H/V Ratio; Ground-Motion Prediction; Seismic Hazard; rock sites.

### INTRODUCTION

It is common for ground motion prediction equations (GMPEs) to be available for predicting horizontal ground-motion given a range of input parameters, such as magnitude, distance and site class. However, in most cases the vertical component of motion is not modelled. For instance, current models based on data from Europe and the Middle East (Akkar and Bommer, 2010); and on the New Generation Attenuation (NGA) dataset (Chiou et al., 2008) all provide only predictions of horizontal ground-motion. However, it has recently been shown that the vertical component of ground-motion can have a significant effect on the seismic response of particular structures, such as bridges (e.g., Kunnath et al., 2008). While it may seem unusual that GMPEs are not typically available for the vertical component, it may actually be beneficial to use a GMPE for the horizontal component of motion in combination with a V/H ratio. In this case, PSHA is undertaken solely on the horizontal component of ground-motion, and resulting design spectra are later adjusted to the vertical orientation. The resulting horizontal and vertical design spectra will then both correspond to exactly the same earthquake (disaggregation) scenario (Gülerce and Abrahamson, 2011).

Newmark and Hall (1969, 1982) were among the first to propose a ratio for the scaling of vertical to horizontal ground-motions. They proposed a V/H ratio of 2/3, independent of period, magnitude, distance and site condition. McGuire et al. (2001) proposed V/H ratios for rock sites in the US based on existing GMPEs (Western US) and stochastic simulations (Central and Eastern US). Their model was given as a function of PGA in rock, such that increasing ground-motion led to higher V/H ratios. For the Western US model they also noted a transition between around 2 and 15 Hz, where the V/H ratio increases from lower values at long periods, to higher values at short periods. Since then, several studies have been undertaken with increasing model complexity, including the use of  $V_{s30}$ : e.g.,

Bozorgnia and Campbell (2004), Cauzzi and Faccioli (2008), Bommer et al. (2011), Gülerce and Abrahamson (2011).

Recently, a novel approach to define a reference rock-velocity condition was developed by Poggi et al. (2011). They correlated empirical shear-wave site amplification (e.g., Edwards et al., 2008) to the quarter-wavelength velocity profile of the site. Using the quarter-wavelength approach to compute average S-wave velocities introduced the possibility of analysing amplification at different frequencies separately. In an extension of this work, soon to be published as Edwards et al. (in press) we investigate the V/H ratio in terms of its relation to the average rock properties using the quarter-wavelength approximation for frequencies much lower than  $f_0$ . On the assumption that for a rock site, the V/H ratio is controlled by characteristics of the shear-wave velocity profile, the resulting correlation between the quarter-wavelength velocity and V/H facilitates the prediction of V/H or equally, H/V, given any specific rock velocity profile. Our interpretation is limited to hard-rock sites, which are of principal interest in PSHA, when rock ground-motions are investigated. V/H ratios due to low-velocity superficial deposits are not considered as they introduce the additional complexity of resonance within the frequency band of interest.

## V/H RATIO DATA

In this paper, we present the analysis of V/H ratios of ground-motion in terms of the 5% damped response spectra. One Swiss and one Japanese dataset are processed following the same method. The time series used are instrument corrected and include various amounts of pre-event noise for SNR testing. Recorded events of any magnitude, occurring at depths of less than 25 km in Japan are included. We imposed a 25km depth limit due to the complex tectonic environment in Japan, such that all events in our dataset can be considered shallow crustal earthquakes. In Switzerland all earthquakes are considered shallow crustal events (with maximum depths of around 33km). Due to the drastically different level of seismic activity in the two regions, each dataset is covered by a different range of magnitudes. The wide overall range of recorded magnitudes ( $M_w=2$  to 7.3) allows us to investigate the magnitude dependence of the V/H ratio.

For each record, the horizontal component used for the V/H ratio is computed from the geometrical mean of the two perpendicular horizontal response spectra. For each recording station,  $m$ , the average V/H ratio is then given by:

$$\log[(\overline{V/H})_m(f)] = \frac{1}{N(f)} \sum_{n=1}^{N(f)} \log [(V/H)_n(f)] \quad 1$$

where  $V$  is the vertical component, and  $H$  is the geometrical mean of two perpendicular horizontal components of the 5% damped response spectrum,  $n$  denotes the  $n$ th record of station  $m$  and  $N(f)$  is the number of records available for a particular frequency at station  $m$ . Examples of V/H Spectra are given in *Fig. 1*.

## VELOCITY PROFILES AND THEIR QUARTER WAVELENGTH REPRESENTATION

A shear-wave velocity profile of each of the 689 stations of the Kik-Net strong-motion network was provided by the Japanese National Research Institute for Earth Science and Disaster Prevention (NIED). These profiles have been obtained from downhole logging on boreholes set up for buried sensor installation (Fujiwara et al., 2004). The maximum depth reached is very variable, depending on the particular station and spans from a few tens of meters to about 200m. Each profile consists of a limited number of discrete layers (generally from 4 to 7), for which an estimate of the S and P velocities is provided. There is a wide range of surface velocity types, from soil to very hard rock. Of these sites, 498 were used in this study, with selection based on  $\frac{1}{4}$  wavelength velocities greater than 800m/s. Unfortunately, an estimation of uncertainties was not provided for the Japanese profiles.

Twenty-six seismic stations of the Swiss Digital Seismic Network (SDSNet, Deichmann et al., 2010) were also used for this study. The sites were investigated as part of the PEGASOS Refinement Project (PRP), a seismic hazard assessment project coordinated by *swissnuclear*, and a microzonation project in the Basel area (e.g., Fäh and Huggenberger, 2006). The locations of the sites investigated during PRP were defined in order to sample the most typical rock site conditions of seismic stations in the Swiss Alpine Foreland. Of the selected station locations, 10 were investigated using three-component high-resolution f-k analysis (Capon (1969) and Poggi and Fäh (2010)), while the rest were investigated using multichannel analysis of surface waves (Park et Al., 1999). For more detailed discussion and analysis of the derivation of the velocity profiles for the Swiss instrumental sites, please refer to Poggi et al. (2011) and references therein.

The quarter-wavelength velocity profiles for the Swiss and Japanese sites are computed following Joyner et al. (1981). The reader is

referred to Poggi et al. (2011) for a complete description of the method.

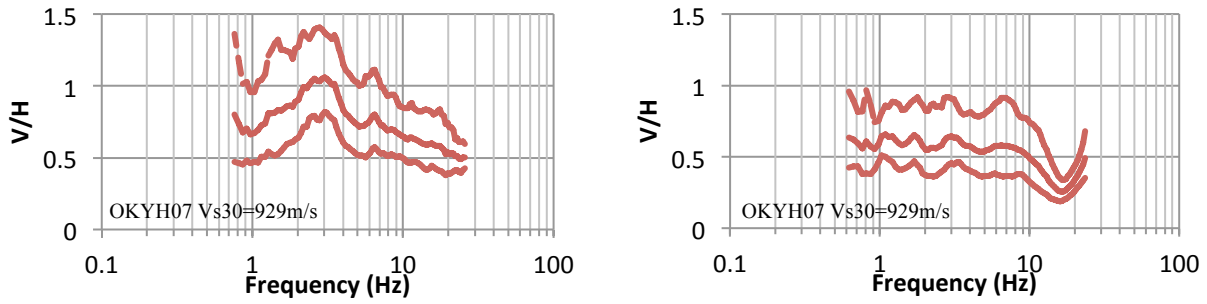


Fig. 1: Response spectra  $V/H$  spectral ratios for two Japanese stations used in the study. Central line: mean; dashed outer lines:  $\pm$  one standard deviation. The minimum and maximum frequencies were limited by the SNR of the earthquake recordings.

The investigation of increasingly long-period (and thus wavelength)  $V/H$  ratio values requires the knowledge of increasingly deep velocity profiles. However, each site is characterized only to a limited depth, depending on the investigation technique employed. It is therefore necessary to extrapolate the required information from the available data below this limit. Adding new layers to the existing velocity models, e.g., using some gradient or power-law function, would involve numerous assumptions. To produce a justifiable estimation we therefore proceed as follows: the quarter-wavelength velocity functions are computed down to a frequency ( $f^{Max}$ ) corresponding to a maximum available profile depth. The thickness of the last layer is usually undefined in the model, so we generally impose a lower depth bound, corresponding to a percentage of the second-to-last layer depth (here 50%). The derived quarter-wavelength profile is then extended to lower frequencies through cubic interpolation of the existing points (Fig. 2). A clear advantage of this procedure is that such an extrapolation produces a smooth average velocity profile, which is constrained by the velocity variation of the uppermost layers. We define an empirical frequency range of validity ( $f^{Ext}$ ) for the extended quarter-wavelength profile, such that:

$$f^{Max} > f^{Ext} \geq 0.5 f^{Max} \quad 2$$

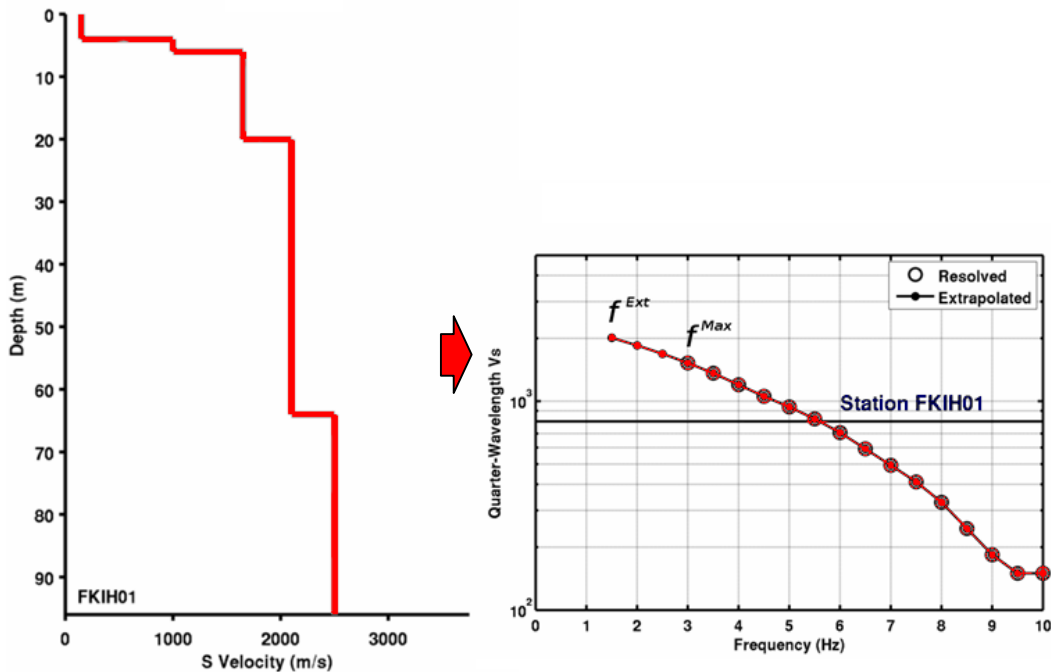


Fig. 2: example of quarter wavelength velocity versus frequency for a profile of the Japanese KiKNet network (right), along with the corresponding shear wave velocity profile (left). The 800m/s velocity threshold for inclusion in the regressions is indicated as a horizontal black line.

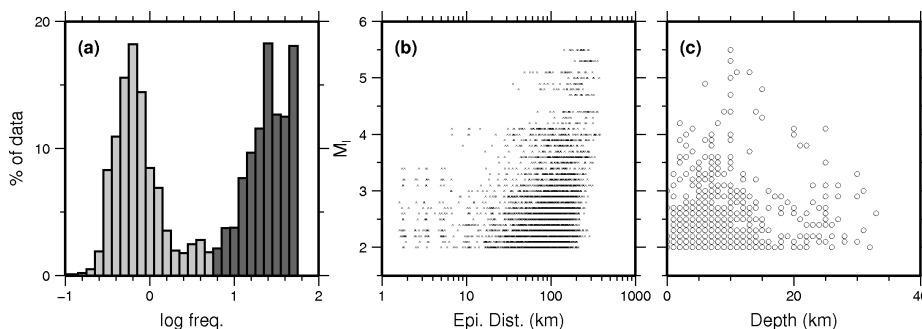
## CORRELATION OF V/H WITH ¼ WAVELENGTH VELOCITY

V/H ratios of 5% damped response spectra (pseudo-spectral acceleration) were compared with the corresponding ¼ wavelength velocity over frequencies from 0.5 to 20Hz. For inclusion in the regression of V/H ratio versus ¼ wavelength velocity, the V/H measure needed to be based on at least 5 records, whilst the ¼ wavelength velocity had to be greater than or equal to 800ms<sup>-1</sup>. This lower limit of ¼ wavelength velocity is defined in order to separate the different contributions of soft sediments and rock sites in the correlation. At the lowest frequencies a limiting factor for data availability is the maximum depth of the velocity profile, while for the highest frequencies it is the resolution of the upper layers' velocities. A regression for the best fitting linear relation between the logarithms of ¼ wavelength velocity and V/H ratio was performed using a least-squares minimization. The form of the equations was:

$$\ln\left(\frac{V}{H}(f)\right) = a(f)\ln(V_s^{QWL}(f)) + b(f) \quad 3$$

5,384 records were used to define the V/H ratios of the 26 Swiss sites used in the regression. Minimum available frequencies ranged from 0.1 to around 10Hz, whilst maximum frequencies ranged from 5 to 50Hz, depending on the noise present in the recording (Fig. 3a top). The recordings sampled a wide range of hypocentral distances, spanning 5 to 300km (Fig. 3b top). Earthquakes with magnitudes between 2 and 5.5 and depths between 0 and 33km were used (Fig. 3c top). The Japanese dataset includes significantly more data than the Swiss. 78,419 records were used to compute the V/H ratios of 498 sites which included ¼ wavelength velocities of greater than 800m/s. The maximum frequency was limited to 30Hz, due to the low-pass filter applied at the recording site (Aoi et al., 2004). The resulting range of frequencies available in the data, after checking the SNR, was between 0.1 and 30Hz (Fig. 3a bottom). The lower bound ranged from 0.1 to around 5Hz, whereas the upper bound ranged from 5 to 30Hz. 3379 events with  $M_{JMA}$  (Japanese Metrological Agency magnitude) between 1.9 and 7.3 were used (Fig. 3b bottom), with hypocentral depths ranging from 0 to 25km (Fig. 3c bottom). A trend of increasing minimum epicentral distance with magnitude is present (Fig. 3b), as often seen due to triggering, occurrence rates and SNR constraints.

Swiss Data:



Japanese Data:

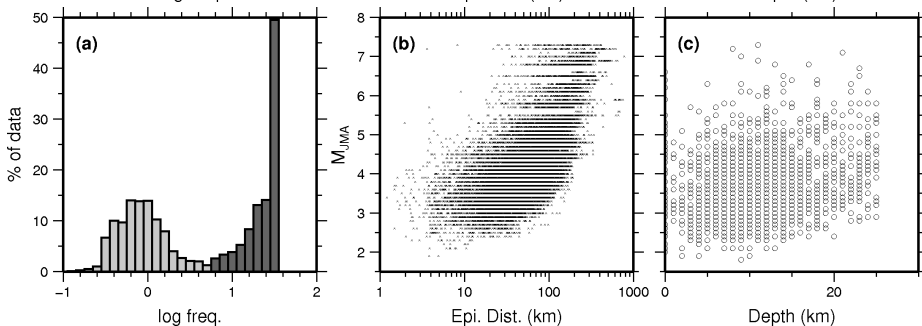


Fig. 3: Data coverage in terms of (a) frequency range (light: minimum; dark: maximum frequency), (b) epicentral distance and (c) earthquake depth for the recordings used to define the V/H ratio of the sites.

An example of the correlation between ¼ wavelength velocity and V/H ratio of 5% damped response spectral amplitude for the Japanese sites is plotted in Fig. 4 for frequencies 1 and 5Hz. Frequencies between 4 and 8Hz tended to lead to the smallest standard deviations relative to the regression. It is possible that this is due to the resolution of the S-wave velocity profiles from MASW analysis used in this study. For instance, an average velocity of 800ms<sup>-1</sup> down to 50m corresponds to the lower 4Hz frequency in the ¼ wavelength representation. Greater depths, with velocities becoming less well resolved by the MASW analysis, correspond to lower frequencies. For frequencies above 8Hz we increasingly enter the limited resolution of the uppermost layers of the velocity profile. Frequencies above this range were considered unreliable: the unreliable velocity profile at depth leads to uncertainty at low

frequencies, whereas the limited amount of data-points with velocity higher than 800m/s in the upper layers in addition to the limited resolution of the velocity profiles in the uppermost layer leads to uncertainty at high frequencies.

The regression results of frequencies up to 10Hz converge at  $\frac{1}{4}$  wavelength velocities around 2000m/s. All fits have a positive gradient, with the V/H ratio changing from around 0.5 at 800m/s to 0.9 at 2500m/s. The general trend for the Japanese data, as with the Swiss data, is for increasing  $\frac{1}{4}$  wavelength velocity to lead to higher V/H ratio over all frequencies. A systematic variation in the results with frequency can be observed. However, in the Japanese case the trend is in the opposite sense to the Swiss, with higher frequencies leading to lower V/H ratios. For the Japanese data all frequencies approach a common ratio of around 0.7 for  $\frac{1}{4}$  wavelength velocities of 2000ms<sup>-1</sup>. This is lower than the value of 0.9 at the same  $\frac{1}{4}$  wavelength velocity seen for the Swiss sites. For lower  $\frac{1}{4}$  wavelength velocities the V/H ratio decreases, down to around 0.4 at 800ms<sup>-1</sup>.

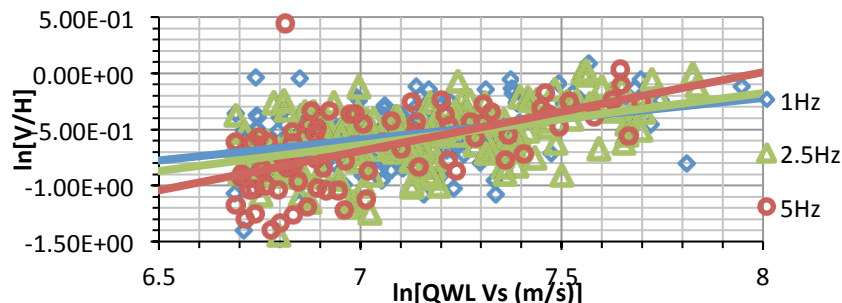


Fig. 4: Correlation of V/H ratio of 5% damped response spectra and  $\frac{1}{4}$  wavelength velocity (in m/s) for the Japanese dataset at selected frequencies.

#### FREQUENCY-INDEPENDENT CORRELATION OF $\frac{1}{4}$ WAVELENGTH AND V/H RATIO

Statistical tests undertaken (Edwards et al., in press) suggest that between around 1 and 7Hz a unique model exists that can explain the relation between V/H and the  $\frac{1}{4}$  wavelength velocity in both the Swiss and Japanese datasets. As the frequency dependence of the V/H relation was in the opposite sense for the two regions, it can also be inferred that a frequency independent relation should fit the combined data equally well in this frequency range. Such a model has the advantage that it is also easy to implement. The form is given by:

$$\ln\left(\frac{V}{H}(f)\right) = a \ln(V_S^{QWL}(f)) + b \quad 4$$

In the following, we produce a frequency independent V/H –  $\frac{1}{4}$  wavelength velocity relation for the individual regions, in addition to a combined average model. To reduce bias in the results, which may occur due to the fact that the data coverage of both low and high frequencies is reduced, a synthetic dataset was produced, based on the individual frequency regressions. For the average model, based on data from both Japan and Switzerland, the resampled dataset also reduces the bias due to the significantly larger size of the Japanese dataset. Resampling of the datasets was made at 10  $\frac{1}{4}$  wavelength velocities between 800 and 2500m/s. 1000 predictions were made at each  $\frac{1}{4}$  wavelength velocity for frequencies 1 to 7Hz in steps of 0.5Hz. A random component was introduced in order to account for the standard deviation of the original regression. The resulting data were then inverted for a frequency independent relation between  $\frac{1}{4}$  wavelength velocity and the V/H ratio. The regression results are given in Table 1. The variation between the Swiss and Japanese results mimics the differences discussed for the frequency dependent regressions, whilst the combined model provides an intermediate model.

Table 1: Regression results for frequency independent Response spectra V/H –  $\frac{1}{4}$  wavelength velocity relation in the form of Equation 4.  $\sigma(\ln)$  is the natural log standard deviation of the regression.

Swiss			Japan			All		
a	b	$\sigma(\ln)$	a	b	$\sigma(\ln)$	a	b	$\sigma(\ln)$
0.584	-4.631	0.238	0.498	-4.163	0.314	0.541	-4.397	0.291

## RESIDUAL MISFIT AND V/H DEPENDENCE ON MAGNITUDE AND DISTANCE

Among others, Gülerce and Abrahamson (2011), Bommer et al. (2011) and Bozorgnia and Campbell (2004) presented models for the V/H ratio based on a range of parameters such as earthquake magnitude, slip type, rupture distance and site characterization in terms of Vs30. Gülerce and Abrahamson found that, in addition to Vs30, the V/H ratio was dependent on the recording distance, and weakly dependent on magnitude. In order to assess if this dependence was present in our data, we performed residual analysis on the back-computed V/H functions for all sites with points having a  $\frac{1}{4}$  wavelength velocity greater than  $800\text{ms}^{-1}$ . Using the predicted V/H ratios, we could compare a range of recorded V/H ratios, at different magnitudes and distances, to the expectation. Any dependence should then be evident in residual plots (e.g., Fig. 5).

We found no evidence for magnitude dependence of the V/H ratio. It should be noted that due to the different magnitude scales employed by the Swiss and Japanese agencies, there may be systematic differences in M between the two datasets. However, the only consequence of this to the residual plot is that densities could be shifted horizontally (M changes). As there is already no trend present with magnitude this could not affect our interpretation. On the other hand, the response spectra V/H show a slight trend with distance. At 30km the V/H ratios are about 5% lower, whereas at 190km, the V/H ratios are, on average, about 5% higher than the model predicts. This trend is, however only present in the Japanese data. Nevertheless, considering the standard deviation, the variation is so small that it should not be over-interpreted. At near-source hypocentral distances ( $R_{\text{hyp}} < 30\text{km}$ ), the variation of V/H with distance is more pronounced for response spectra, with V/H around 18% lower than the model at 10km. A correction for this near-field effect ( $\delta_r$ ) was computed by producing a linear fit to the mean V/H residual versus distance within 30km. This led to:

$$V/H_{RCorr} = \delta_r \frac{V}{H} = 10^{(4.13 \cdot 10^{-3} R_{\text{hyp}} - 0.127)} \frac{V}{H} \quad R_{\text{hyp}} \leq 30\text{km} \quad 5$$

As we now use the frequency independent regression model, the residuals are not forced to have zero mean at all frequencies. In order to improve the high frequency fit of the frequency independent correlation model further, we propose a simple adjustment ( $\delta_f$ ) based on the residual analysis, such that:

$$V/H_{hfCorr} = \delta_f \frac{V}{H} = \frac{(V/H)}{0.722 + 0.9672 \exp(-0.176f)} \quad f > 7\text{Hz} \quad 6$$

This correction is consistent with the results of others such as McGuire et al. (2001), Gülerce and Abrahamson (2011) and Bommer et al. (2011), who also found higher V/H at frequencies greater than approximately 10Hz. The final residual misfit of the data to the V/H model is shown in Fig. 5. The correction for the response spectra in the near field (Equation 5) and the high-frequency correction (Equation 6) are applied. Even well beyond the frequencies used in the combined frequency regression (1-7Hz), and up to 25Hz (limited by the data bandwidth) the residual misfit is still reasonable.

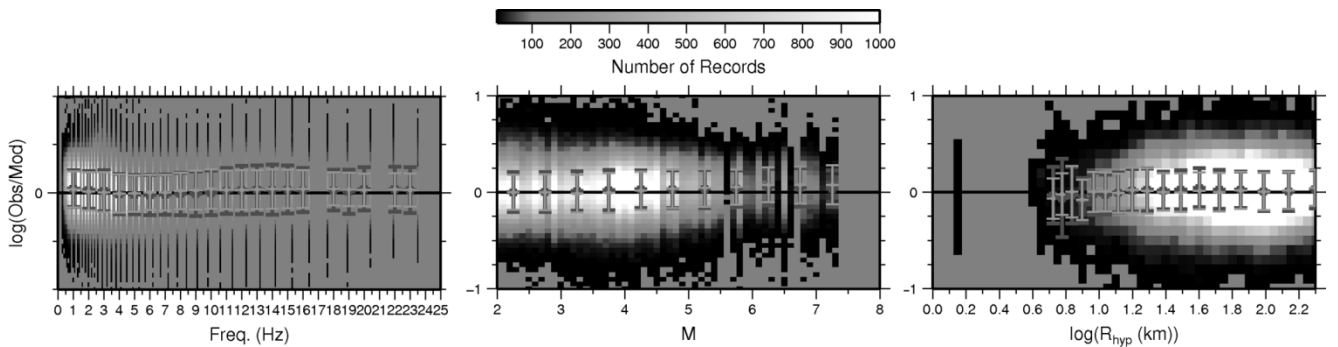


Fig. 5: Residual analysis of recorded V/H (labelled Obs) versus V/H reconstructed using the frequency independent V/H -  $\frac{1}{4}$  wavelength velocity relation (labelled Mod) for the V/H data. The corrections for near-field response spectra V/H (Equation 5) and high frequency V/H (Equation 6) are applied. The error bars indicate the mean and standard deviation of the residuals.

## COMPARISON WITH OTHER MODELS

Fig. 6 shows a comparison of the combined V/H model with the models of Gülerce and Abrahamson (2011), Bommer et al. (2011) and Campbell and Bozorgnia (2003) for a  $M_w=6.0$  at 30km on the generic rock Vs profile of Poggi et al. (2011). The match is good in this case, with increasing V/H with  $\frac{1}{4}$  wavelength velocity (lower frequency). However, for very hard-rock (e.g., bedrock conditions often used in PSHA) the models deviate, as the GMPE type-models are unconstrained and extrapolate into the hard-rock parameter space. However, in the range of rock velocity 800-1200m/s the models do consistently fall within the standard deviation of one another.

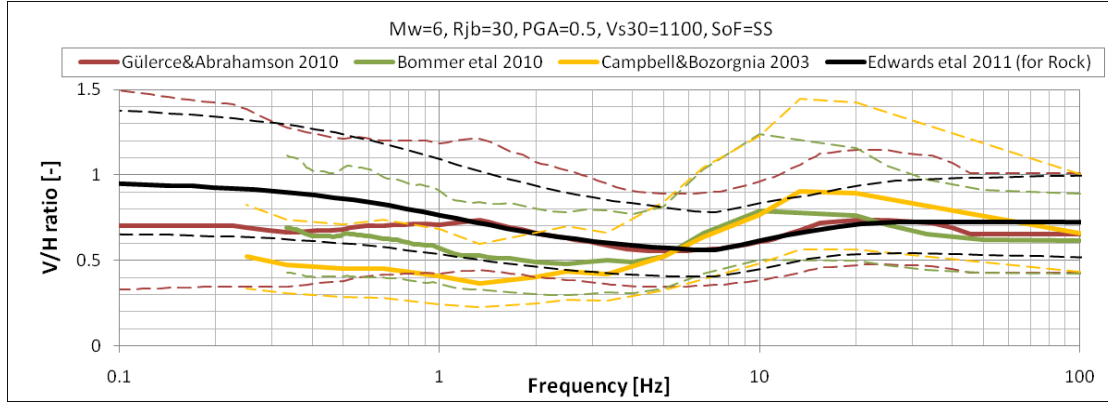


Fig. 6: comparison between the Combined frequency independent V/H –  $\frac{1}{4}$  wavelength velocity relation models for Response Spectra and the models of Gülerce and Abrahamson (2011), Bommer et al. (2011) and Campbell and Bozorgnia (2003) for the Swiss generic Rock Vs model of Poggi et al (2011) ( $V_{s30}=1100\text{m/s}$ ). The standard deviation ( $\pm$  sigma) is indicated by the dashed lines.

## CONCLUSIONS

We showed that, in the log-space, the V/H ratio at a given frequency was linearly related to the corresponding site's  $\frac{1}{4}$  wavelength velocity over a suite of over 450 Japanese, and 26 Swiss sites. A frequency independent parameterisation of the relation was presented. In addition, a correction for V/H of near-field response spectra and V/H at high frequencies was included, purely based on observational misfit to the initial  $\frac{1}{4}$  wavelength model. The model is completely independent of earthquake magnitude. The final V/H model, including single site uncertainty ( $\sigma_{SS}$ , see Edwards et al. (in press)), is:

$$\ln\left(\frac{V}{H}\right) = \ln(\delta_r \delta_f) + \left[ a \ln(V_s^{QWL}) + b \right] \pm \sigma_{SS} \quad 7$$

With:

$$\begin{aligned} \delta_r &= 10^{(4.13 \cdot 10^{-3} R_{hyp} - 0.127)} && \text{for response spectra with } R_{hyp} \leq 30\text{km} \\ \delta_r &= 1 && \text{for response spectra with } R_{hyp} > 30\text{km} \\ \delta_f &= 1 && \text{for } f \leq 7\text{Hz} \\ \delta_f &= \frac{1}{0.722 + 0.9672 \exp(-0.176f)} && \text{for } f > 7\text{Hz} \end{aligned}$$

with a and b given by the combined model in Table 1.

The magnitude and distance dependence of the V/H ratio was also explored. Moment magnitudes between 2 and 7.3, and distances up to 200km were tested. We compared the measured V/H ratio with the model and found that, contrary to other models, there was no systematic dependence on with either magnitude. However, for near-source distances ( $R < 30\text{km}$ ) the response spectra V/H were generally lower than the initial distance independent model.

Some differences in V/H existed when analysing the Swiss and Japanese datasets. One explanation for this difference could be the composition of the wave-fields, related the peculiarities of the sites in the particular region. For example, the influence of sedimentary basins and topography. Swiss sites have a tendency to be close to a theoretical rock sites where body waves, in particular P-waves, might contribute more to the wave-field at high frequency, whereas Japanese sites include a number of sites close to or in deep basins in which surface wave excitation might significantly contribute to the wave-field. A further reason for the small differences in V/H could be a measurement bias of the velocity profiles in the two datasets.

## ACKNOWLEDGEMENTS

We thank the NIED for making waveform and velocity profile data available. This work was funded partly by *swissnuclear* and the Swiss Federal Nuclear Safety Inspectorate (ENSI).

## REFERENCES

- Akkar, S. & J. J. Bommer, [2010]. Empirical Equations for the Prediction of PGA, PGV and Spectral Accelerations in Europe, the Mediterranean Region and the Middle East, *Seismological Research Letters*, 81(2), 195-206.
- Aoi, S., T. Kunugi and H. Fujiwara [2004]. Strong-Motion Seismograph Network Operated by NIED: K-Net and KiK-Net, *Journal of Japan Association for Earthquake Engineering*, Vol. 4, No. 3 (Special Issue).
- Bommer, J.J., S. Akkar & Ö. Kale [2011]. A model for vertical-to-horizontal response spectral ratios for Europe and the Middle East. *Submitted to Bulletin of the Seismological Society of America*.
- Bozorgnia, Y. & K.W. Campbell [2004]. The vertical-to-horizontal spectral ratio and tentative procedures for developing simplified V/H and vertical design spectra. *Journal of Earthquake Engineering* 4(4), 539-561.
- Capon, J. [1969]. High-resolution Frequency-wavenumber Spectrum Analysis. *Proceedings of the IEEE*, 57, 1408-1418.
- Cauzzi, C. & E. Faccioli (2008). Broadband (0.05 to 20 s) prediction of displacement response based on worldwide digital records. *Journal of Seismology* 12, 453-475.
- Chiou, B., R. Darragh, N. Gregor, and W. Silva [2008]. NGA project strong-motion database, *Earthquake Spectra* 24, 23—44.
- Deichmann et al., [2010]. Earthquakes in Switzerland and surrounding regions during 2009. *Swiss Journal of Geosciences*.
- Edwards, B., A. Rietbrock, J. J. Bommer, and B. Baptie [2008]. The Acquisition of Source, Path and Site Effects from Micro-earthquake Recordings using Q Tomography: Application to the UK, *Bull. Seism. Soc. Am.*, 98, 1915–1935.
- Edwards, B., V. Poggi and D. Fäh (in press). A Predictive Equation for the Vertical-to-Horizontal Ratio of Ground Motion at Rock Sites Based on Shear-Wave Velocity Profiles from Japan and Switzerland. *Bull. Seism. Soc. Am.*
- Fäh, D. and P. Huggenberger [2006]. INTERREG III, Erdbebenmikrozonierung am südlichen Oberrhein. Zusammenfassung für das Projektgebiet Gebiet in der Schweiz. CD and Report (in german; available from the authors).
- Fujiwara, H., S. Aoi, T. Kunugi, and S. Adachi [2004]. Strong-motion observation networks of NIED: K-NET and KIK-net. [http://www.cosmos-eq.org/events/wkshop\\_records\\_processing/papers/Fujiwara\\_paper.pdf](http://www.cosmos-eq.org/events/wkshop_records_processing/papers/Fujiwara_paper.pdf), COSMOS (last accessed January 2011).
- Gülerce, Z. and N. Abrahamson, [2011]. Site-Specific Design Spectra for Vertical Ground-Motion, accepted for publication in *Earthquake Spectra*.
- Kunnath, S.K., E. Erduran, Y.H. Chai and M. Yashinsky (2008). Effect of near-fault vertical ground motions on seismic response of high overcrossings, *Journal of Bridge Engineering*, 13, 282-290.
- Joyner, W. B., R. E. Warrick, and T. E. Fumal [1981]. The effect of Quaternary alluvium on strong ground motion in the Coyote Lake, California, earthquake of 1979, *Bull. Seism. Soc. Am.* 71, 1333-1349.



McGuire, R.K., W.J. Silva & C.J. Costantino [2001]. Technical basis for revision of regulatory guidance on design ground motions: Hazard- and risk-consistent ground motion spectra guidelines. *NUREG/CR-6728*, US Nuclear Regulatory Commission, Washington D.C.

Newmark, N.M. & W.J. Hall [1969]. Seismic design criteria for nuclear reactor facilities. *Proceedings of 4th World Conference on Earthquake Engineering*, Santiago, Chile, B4:37-50.

Newmark, N.M. & W.J. Hall [1982]. Earthquake Spectra and Design. *EERI Monograph*, Earthquake Engineering Research Institute, Oakland, California.

Park C. B., R. D. Miller and J. Xia, [1999]. Multichannel analysis of surface waves, *Geophysics*, 64, 800-808.

Poggi, V., B. Edwards, and D. Fäh., [2011]. Derivation of a Reference Shear-Wave Velocity Model from Empirical Site Amplification, *Bull. Seis. Soc. Am.* **101**, 258-274.

Poggi, V. and Fäh, D. [2010], Estimating Rayleigh wave particle motion from three-component array analysis of ambient vibrations. *Geophysical Journal International*, 180: 251–267. doi: 10.1111/j.1365-246X.2009.04402.x.